Biophysical Chemistry 12 (1980) 243–253

THEORETICAL MODELS FOR THE COVALENT ASSEMBLY OF IMMUNOGLOBULINS

V.L. HESS and Attila SZABO ‡
Department of Chemistry, Indiana University, Bloomington, Indiana 47405, USA

Received 10 March 1980

Theoretical models for the formation of interchain disulfide bonds in noncovalently assembled immunoglobulin molecules are presented. The formalism handles independent and cooperative bond formation with equal ease. Analysis of certain experimental results on the covalent assembly of human immunoglobulin G yields information about the pathway of assembly. A model in which the formation of bonds between the light and heavy chains is independent of, but twice as fast as, those between two heavy chains, gives satisfactory agreement with these results. Simple models involving cooperative bond formation are also considered, but the experiments being analyzed are not accurate enough to unambiguously implicate any cooperative pathway.

1. Introduction

A good deal of experimental work has been directed toward the elucidation of the mechanism by which the two light (L) chains and the two heavy (H) chains of immunoglobin G (IgG) assemble to form the active molecule (H_2L_2). Kinetic evidence indicates that the noncovalent interactions are established rapidly. This noncovalent assembly is followed by covalent assembly: i.e. the formation of four interchain disulfide bridges. In an interesting series of papers, Beychok and coworkers [1,2] set out to establish the pathway of covalent assembly by monitoring the appearance of intermediates during the formation of disulfide bonds in noncovalently assembled IgG.

Briefly, these experiments entailed reducing the interchain disulfide bonds of IgG under conditions which leave noncovalent interactions intact, and then changing conditions to allow the bonds to form again. Periodically, aliquots were removed from the system and analyzed to determine the average number of bonds formed per molecule and the concentrations of the various fragments obtained by breaking only noncovalent interactions. Since the experimental technique did not distinguish between the presence of one HH bond and two, there were six fragments whose concentrations could be measured: L, H, LH, H_2, H_2L, and H_2L_2. Plots of fragment concentrations (expressed as mole fractions of the total amount of protein present) versus the average number of bonds formed per molecule gave a profile of the reaction process.

In order to use these data to determine whether interchain bonds form independently or cooperatively, Sears and Beychok [3] presented a theoretical framework based on probability theory. Their approach easily handled the situation in which HH and LH bonds form independently and with equal ease, but ran into serious difficulties when these bonds formed with different probabilities even in the absence of cooperativity.

The purpose of this paper is to present a theoretical framework, free from these difficulties, which can be used to extract information about the pathway of covalent assembly from the experimental data. The theory uses first order kinetics, and can handle cooperative and independent bond formation with equal ease. In the special case of noncooperative bond formation, a connection is made with the probabilistic scheme of Sears and Beychok [3]. When HL and HH bonds form with equal ease, the results obtained are identical to theirs. However, when the HL and HH bonds form at different rates, our formalism avoids the problems associated with their probabilistic approach.

‡ Alfred P. Sloan Research Fellow.

At this point it is appropriate to discuss another approach to the kinetics of covalent assembly of immunoglobulin. Percy and coworkers [4–7] have used a formalism based on second order rate theory to describe disulfide bond formation. Their theory differs from ours in two respects: (1) their rate equations are written in terms of the fragment concentrations, whereas ours are written in terms of the concentrations of noncovalently assembled aggregates at various stages of disulfide bond formation, and (2) they assume that bond formation can be described by the same set of second-order equations whether or not noncovalent assembly has already taken place (i.e. whether or not fragments are free to choose their collision partners) whereas we assume a first order rate law for disulfide bond formation in the already noncovalently assembled molecule. It should be noted that the fragment concentrations we obtain do not obey a simple rate law. The second-order model semiquantitatively described their experiments [4–6], which, due to differing experimental conditions, are not directly comparable to those of Sears et al., which are the primary concern this paper. However, we do discuss some preliminary results indicating that our formalism is a viable alternative to the second-order formulation in describing the experiments of Percy et al. [5–7] ‡.

The outline of the paper is as follows: in section 2, we set up the appropriate first order equations. Since the experimental conditions strongly favor the formation of disulfide bonds over their dissociation at every stage, we make the simplifying assumption that the reactions are irreversible. The general reaction scheme does not distinguish between the two HH bonds, even though these are structurally different, since these experiments do not allow such a distinction. In section 3, we develop a simple probabilistic approach which allows us to write down the solutions of the rate equations by inspection for any noncooperative model. We also discuss the connection with the work of Sears and Beychok [3]. In section 4, we use both cooperative and noncooperative models to analyze the experiments of Sears et al. [1,2]. Finally, in section 5, we discuss the applicability of our formalism to the work of Percy et al. [4–7] and suggest future lines of investigation.

‡ Percy and coworkers [7] do present evidence that in an unusual "half-molecule" myeloma protein the reoxidation of a single category of interchain disulfide bridge, the inter H–L bond, follows an apparent second-order rate law. However, the evidence does not appear to be conclusive since the concentrations of light and heavy chains have different time dependence (see their figure 4B). This indicates that the situation must be more complex than they have assumed and first-order kinetic models cannot be ruled out a priori.

2. General formalism

We wish to use first order rate theory to calculate the concentrations of the species shown in fig. 1, and from these to get the fragment concentrations and the average number of bonds formed. To do this, we write down the rate equations, a series of equations of the form

$$\frac{dc_l}{dt} = \sum_{m=1}^{N} K_{lm} c_m \,, \quad (l = 1, 2, \ldots, N) \,, \tag{1}$$

where the c_l are the species concentrations, the K_{lm} are rate constants for the reactions

$$\text{species } m \rightarrow \text{species } l \tag{2}$$

and K_{ll} is defined by

$$K_{ll} = -\sum_{m \neq l}^{N} K_{ml} \,. \tag{3}$$

This system of equations may be written as a single matrix equation

$$d\boldsymbol{c}/dt = \mathbf{K}\boldsymbol{c} \,, \tag{4}$$

where $\boldsymbol{c}$ is a vector whose elements are the c_l of eq. (1) and $\mathbf{K}$ is the matrix of rate constants. The general solution of such an equation is well known to be

$$\boldsymbol{c}(t) = \exp(\mathbf{K}t)\,\boldsymbol{c}(0) \,. \tag{5}$$

It is useful to express $\boldsymbol{c}(t)$ as a linear combination of eigenvectors ($\boldsymbol{X}^{(j)}$) and eigenvalues (κ_j) of the rate matrix, $\mathbf{K}$, i.e.

$$\mathbf{K}\boldsymbol{X}^{(j)} = \kappa_j \boldsymbol{X}^{(j)} \,. \tag{7}$$

Eq. (7) is equivalent to

$$\mathbf{K}\mathbf{X} = \mathbf{X}\boldsymbol{\kappa} \,, \tag{8}$$

where $\mathbf{X}$ is an $N \times N$ matrix whose columns are the eigenvectors of $\mathbf{K}$ (i.e. $(\mathbf{X})_{ij} = X_i^{(j)}$) and $\boldsymbol{\kappa}$ is a diagonal

matrix containing the corresponding eigenvalues.

From eq. (8) we have

$$\mathbf{K} = \mathbf{X}\boldsymbol{\kappa}\mathbf{X}^{-1} , \tag{9}$$

and, therefore,

$$\exp(\mathbf{K}t) = \mathbf{X}\exp(\boldsymbol{\kappa}t)\,\mathbf{X}^{-1} . \tag{10}$$

The general solution of eq. (1), then, in terms of eigenvalues and eigenvectors of $\mathbf{K}$, is

$$\boldsymbol{c}(t) = \mathbf{X}\exp(\boldsymbol{\kappa}t)\,\mathbf{X}^{-1}\boldsymbol{c}(0) , \tag{11}$$

or, for the individual concentrations,

$$c_l(t) = \sum_{m=1}^{N}\sum_{n=1}^{N} X_{lm}\exp(\kappa_m t)(\mathbf{X}^{-1})_{mn}c_n(0) . \tag{12}$$

At the beginning of the experiment, $c_1 = 1$ and all other concentrations are 0. This requirement can be written

$$c_n(0) = \delta_{n1} , \tag{13}$$

which gives

$$c_l(t) = \sum_{m=1}^{N} X_{lm}\exp(\kappa_m t)(\mathbf{X}^{-1})_{m1} . \tag{14}$$

The above formalism is general. For the problem we are considering, the experimental conditions are such that bond formation is essentially irreversible. This implies that $K_{lm} = 0$ if $l < m$. The rate matrix corresponding, under this assumption, to the reaction scheme shown in fig. 1, is $\mathbf{K}$ (see right column).

The eigenvalues of a triangular matrix are just the diagonal elements: $\kappa_n = K_{nn}$. Now we consider the eigenvectors. From eq. (8) we can infer that

$$(\mathbf{K} - \kappa_n\mathbf{I})\boldsymbol{X}^{(n)} = 0 . \tag{16}$$

Multiplying both sides by $(\mathbf{X}^{-1})_{n1}$ gives

$$(\mathbf{K} - \kappa_n\mathbf{I})\boldsymbol{X}^{(n)}(\mathbf{X}^{-1})_{n1} = 0 . \tag{17}$$

If we define

$$(\boldsymbol{d}^{(n)})_l = d_l^{(n)} = X_l^{(n)}(\mathbf{X}^{-1})_{n1} , \tag{18}$$

we have

$$(\mathbf{K} - \kappa_n\mathbf{I})\boldsymbol{d}^{(n)} = 0 , \tag{19}$$

$$\mathbf{K} = \begin{pmatrix}
-2(k_1+k_2) & 0 & 0 & 0 & 0 & 0 & 0 & 0 & 0 & 0 \\
2k_1 & -(k_3+2k_4) & 0 & 0 & 0 & 0 & 0 & 0 & 0 & 0 \\
2k_2 & 0 & -(2k_5+k_6) & 0 & 0 & 0 & 0 & 0 & 0 & 0 \\
0 & k_3 & 0 & -2k_7 & 0 & 0 & 0 & 0 & 0 & 0 \\
0 & 2k_4 & 2k_5 & 0 & -(k_8+k_9) & 0 & 0 & 0 & 0 & 0 \\
0 & 0 & k_6 & 0 & 0 & -2k_{10} & 0 & 0 & 0 & 0 \\
0 & 0 & 0 & 2k_7 & k_8 & 0 & -k_{11} & 0 & -k_{12} & k_{12} \\
0 & 0 & 0 & 0 & k_9 & 2k_{10} & 0 & 0 & 0 & k_{11} \\
0 & 0 & 0 & 0 & 0 & 0 & 0 & -k_{12} & 0 & 0 \\
0 & 0 & 0 & 0 & 0 & 0 & 0 & k_{12} & 0 & 0
\end{pmatrix} \tag{15}$$

and

$$c_l(t) = \sum_{n=1}^{9} \exp(\kappa_n t) d_l^{(n)} . \tag{20}$$

Finally, we have

$$\sum_{n=1}^{9} d_l^{(n)} = \sum_{n=1}^{9} X_{ln} (\mathbf{X}^{-1})_{n1} = \delta_{n1} , \tag{21}$$

which is the required normalization. Hence, we need to solve eq. (19) subject to eq. (21). The concentrations obtained from this procedure are given in the appendix.

The fragment concentration are obtained from the equation

$$f_i = \sum_{l=1}^{9} c_l n_{il} , \tag{22}$$

that is, the concentration of fragment type i is obtained by multiplying the concentration of each species by the number of i-type fragments it contributes and summing the results. For example, to determine the number of LH fragments, we first look at fig. 1 to find that species 2 contributes one such fragment, species 4 contributes two, and the other species contribute none. Thus,

$$f_{LH} = (1)c_2 + (2)c_4 . \tag{23}$$

Since each protein molecule could contribute two L's, two H's, or two LH's, the concentrations of these fragments are divided in half in order that the maximum concentration plotted for any fragment be 1.

In a similar manner, the average number of bonds is obtained from

$$s = \sum_{l=1}^{9} c_l n_l , \tag{24}$$

where s is the average number of bonds per molecule and n_l is the number of bonds in species l. The general expressions for the fragment concentrations and the average number of bonds, given in terms of the c_l, are in table 1.

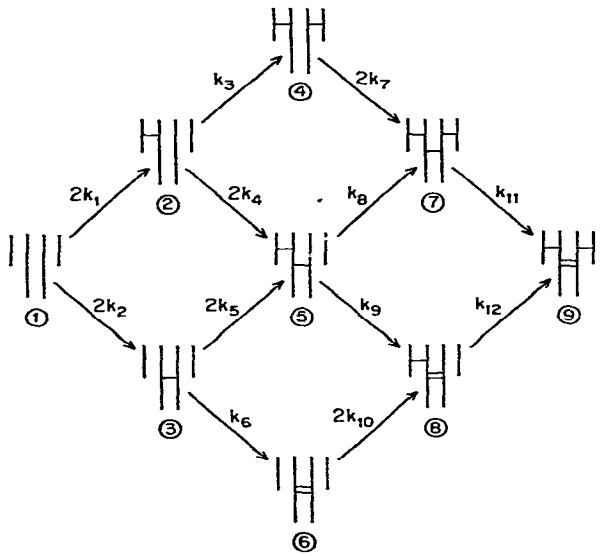

Fig. 1. General kinetic scheme corresponding to the formation of disulfide bonds in noncovalently assembled IgG. The horizontal lines in the diagram represent the disulfide bonds.

3. Probability and simple cases

The concentrations in the experimental plots were expressed as mole fractions of the fragments with respect to the protein in the sample. The probability of observing a particular species is defined in the same way as the mole fraction:

$$P_l = c_l \Big/ \sum_l c_l . \tag{25}$$

where the species referred to correspond to the diagrams in fig. 1. This suggests a close relationship between the solutions to the kinetics equations and probability theory.

We have developed a formalism, based on this rela-

Table 1
Fragment concentrations and the average number of bond(s) expressed in terms of the species concentrations. See text for discussion.

$2f_L = 2c_1 + c_2 + 2c_3 + c_5 + 2c_6 + c_8$

$2f_H = 2c_1 + c_2 , \quad 2f_{HL} = c_2 + 2c_4 , \quad f_{H_2} = c_3 + c_6 ,$

$f_{H_2L} = c_7 + c_9 , \quad f_{H_2L_2} = c_7 + c_9 ,$

$s = (c_2 + c_3) + 2(c_4 + c_5 + c_6) + 3(c_7 + c_8) + 4c_9$

tionship, which can be applied to any number of different types of bonds; the only requirement is that the rate constant governing the formation of a given type of bond not change during the course of the experiment, i.e. that bond formation be noncooperative. This formalism is extremely easy to use and is completely equivalent to the solution of the rate equations by matrix methods.

The concentration of a given empty bond site changes according to the equation

$$dp_i/dt = -k_i p_i \,, \tag{26}$$

which has the solution

$$p_i = A \exp(-k_i t) \,, \tag{27}$$

where A is the initial concentration of empty sites. Each protein molecule has one each of four different bond sites. Since concentrations are expressed as mole fractions of total protein, A is equal to 1. As t varies between 0 and ∞, p_i varies between 1 (all sites of type i unbound) and 0 (all sites of type i bound). The probability of four independent events occurring simultaneously is just the product of their independent probabilities. Hence

$$c_j = g_j \prod_{i=1}^{4} P_{ij} \,, \qquad P_{ij} = \begin{cases} p_i & \text{site empty} \\ 1 - p_i & \text{site bound} \end{cases} \,, \tag{28}$$

where g_j is the number of different ways a species can form. For example, in forming species 3, there are two possible positions for the HH bond; therefore, there are two ways of forming species 3.

The simplest model is one in which all rate constants, and thus all the p_i, are equal. The expressions for the concentrations are extremely simple; for example, the concentration of species three is given by

$$c_3 = 2p^3(1-p) \,. \tag{29}$$

The single bond gives the factor of $1 - p$, the three unbound sites each contribute a factor of p, and the 2 arises because there are two sites at which HH bonds can form. The average number of bonds is obtained by subtracting the number of empty sites from the total number of sites to give

$$s = 4(1-p) \,. \tag{30}$$

The resulting expressions for the c_l are given in table 2.

To extend this formalism to noncooperative models

Table 2
Species and fragment concentrations with all rate constants equal. The fragment concentrations are obtainable from equations in table 1 and take an especially simple form here

$c_1 = p^4$	$f_L = p$
	$f_H = p^3$
$c_2 = 2(1-p)p^3$	$f_{HL} = p^2(1-p)$
$c_3 = 2(1-p)p^3$	$f_{H_2} = p^2(1-p^2)$
	$f_{H_2L} = 2p(1-p)(1-p^2)$
$c_4 = (1-p)^2p^2$	$f_{H_2L_2} = (1-p^2)(1-p)^2$
$c_5 = 4(1-p)^2p^2$	$s = 4(1-p)$
$c_6 = (1-p)^2p^2$	
$c_7 = 2(1-p)^3p$	
$c_8 = 2(1-p)^3p$	
$c_9 = (1-p)^4$	

in which LH and HH bonds form at different rates, we obtain from eq. (27)

$$p_{LH} = \exp(-k_{LH}t) \,, \quad p_{HH} = \exp(-k_{HH}t) \,. \tag{31}$$

If $k_{HH} = x k_{LH}$, we have

$$p_{HH} = p_{LH}^x \,. \tag{32}$$

The species concentrations are obtained as before. For example, to obtain the concentration of species 3 in fig. 1, we note the presence of two unbound LH sites, which together contribute a factor of p_{LH}^2, one unbound HH site, contributing a factor of p_{HH}, and a bound HH site, contributing a factor of $(1 - p_{HH})$. As before, there is a statistical factor of 2. Hence,

$$c_3 = 2p_{LH}^2 p_{HH}(1 - p_{HH}) = 2p_{LH}^{2+x}(1 - p_{LH}^x) \,. \tag{33}$$

The equations giving the c_l, s, and the fragment concentrations are shown in table 3.

When the rates of formation of LH and HH bonds are identical the above formalism is equivalent to that of Sears and Beychok [3]. On the other hand, when the rates differ, our formulation differs. Sears and Beychok assumed that the probabilities, rather than the rate constants, were related by a multiplicative factor (i.e. $p_{HH} = x p_{LH}$ as opposed to eq. (32)). It is clear that it is not possible for both p_{HH} and p_{LH} to

Table 3
Species concentrations when $k_{HH} = x k_{LH}$

$p_{HH} = p_{LH}^{x}$	
$c_1 = p_{LH}^2 p_{HH}^2$	
$c_2 = 2(1 - p_{LH}) p_{LH} p_{HH}^2$	
$c_3 = 2 p_{LH}^2 p_{HH}(1 - p_{HH})$	
$c_4 = (1 - p_{LH})^2 p_{HH}^2$	
$c_5 = 4(1 - p_{LH})(1 - p_{HH}) p_{LH} p_{HH}$	
$c_6 = p_{LH}^2 (1 - p_{HH})^2$	
$c_7 = 2(1 - p_{LH})^2 (1 - p_{HH}) p_{HH}$	
$c_8 = 2(1 - p_{LH})(1 - p_{HH})^2 p_{LH}$	
$c_9 = (1 - p_{LH})^2 (1 - p_{HH})^2$	

vary between 0 and 1 and still satisfy such a relation. Therefore, as Sears and Beychok [3] observed, the ratio of the probabilities would have to be made discontinuous to avoid having the values of the probabilities exceed unity. This difficulty is completely absent in our formalism.

4. Analysis of experiments

In this section we analyze the experiments of Beychok and coworkers [1–3] within the framework of the models described in the previous sections.

4.1. Equal rate constants

The profile obtained using this model is shown in fig. 2a, and is identical to that found by Sears and Beychok [3] for "random reoxidation". Following these authors, we evaluate the resemblance between the experimental and theoretical profiles by comparing the maxima of the LH, HH, and H_2L curves and the locations along the abscissa in terms of $r = 8 - 2s$ (see table 4). The agreement is very poor, indicating that reoxidation does not occur at equal and independent rates.

4.2. Uncqual rates without cooperativity

The profile for this case with $x = 0.5$ (i.e. the rate of HH bond formation is half that of LH bond formation) is shown in fig. 2b, and comparison with experiment is made in table 4: agreement is satisfactory. In this case, our profile is not the same as that obtained by Sears and Beychok [3] for nonrandom but independent bond formation. The unsatisfactory features of their profile (of which the most prominent was the crossing of the abscissa by the L and H_2L curves at $r = 1.33$) resulted from their assumption that the ratio of the probabilities of forming LH and HH bonds was a constant throughout the reaction. (They did note that this ratio was discontinuous, but they did not incorporate that into their calculations.) In our formalism, these difficulties do not arise, since it is the ratio of rate constants (or, equivalently, the ratio of the logarithms of the probabilities) which is held fixed. Despite these differences, Sears and Beychok [3] did arrive at the conclusion that HH bond formation is less likely than LH bond formation. However, it was primarily the unsatisfactory features of their formalism which led them to conclude that some degree of cooperativity was necessary to explain the experimental results.

Table 4
Maxima of H_2, HL and H_2L curves

Model	HL_{max} ($r = 8 - 2s$)	H_{2max} (r)	H_2L_{max} (r)
Experiment	27 ± 4 (4.6 ± 0.7)	18 ± 8 (5.7 ± 1.4)	29 ± 4 (2.8 ± 0.7)
Noncooperative			
$x = 1.0$	15 (5.4)	25 (5.7)	40 (3.1)
$x = 0.5$	25 (4.8)	15 (5.9)	30 (3.6)
Cooperative Model II:			
$x = 0.5, a = 0.8$	25 (4.9)	16 (5.8)	32 (3.4)

4.3. Cooperativity

Although our model for unequal but independent rates for LH and HH bond formation agrees with experiment reasonably well, we did investigate whether introducing cooperativity would further improve agreement.

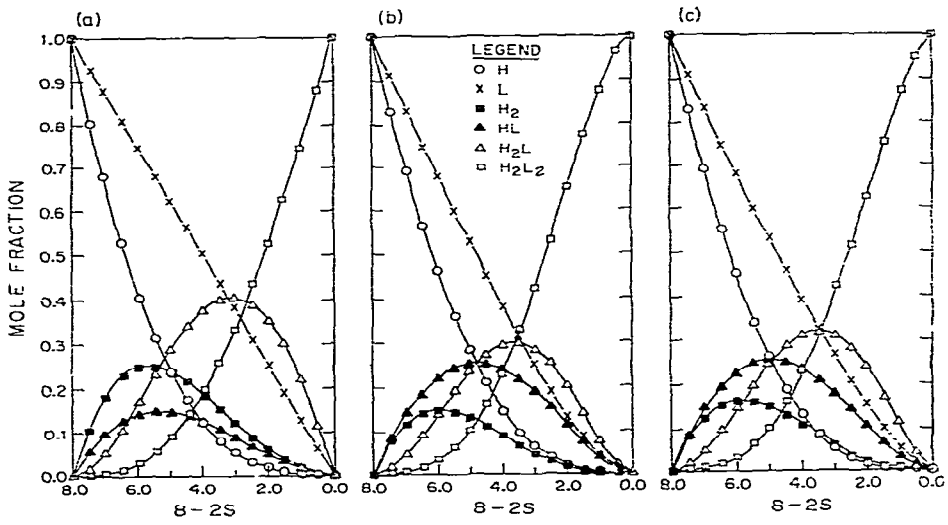

Fig. 2. Fragment concentrations versus $r = 8 - 2s$. a) All rate constants equal; b) $k_{HH} = 0.5k_{LH}$, binding independent; c) Cooperative Model II (see text), $x = 0.5$, $a = 0.8$.

The simplest form of cooperativity is one in which there exists only one type of interaction. There are four possibilities:

1. LH bonds affecting the formation of other LH bonds;
2. LH bonds affecting the formation of HH bonds;
3. HH bonds affecting the formation of LH bonds;
4. HH bonds affecting the formation of other HH bonds.

The first two possibilities are combined in Model I, the third is represented separately in Model II, and the fourth is neglected, since it is not possible to distinguish experimentally between the presence of one HH bond and two.

Model I is described by

$$k_{LH} = k_1 = k_5 = k_{10} ,$$

$$k_{HH} = k_2 = k_6 = xk_1 ,$$

$$ak_{LH} = k_3 = k_8 = k_{12} = ak_1 ,$$

$$bk_{HH} = k_4 = k_7 = k_9 = k_{11} = bxk_1 . \qquad (34)$$

The corresponding reaction scheme is shown in fig. 3. To test possibility 1, b was set equal to 1 and a was varied; to test possibility 2, a was set equal to 1 and b was varied. Neither possibility gave results in better agreement with experiment than the noncooperative model with $x = 0.5$.

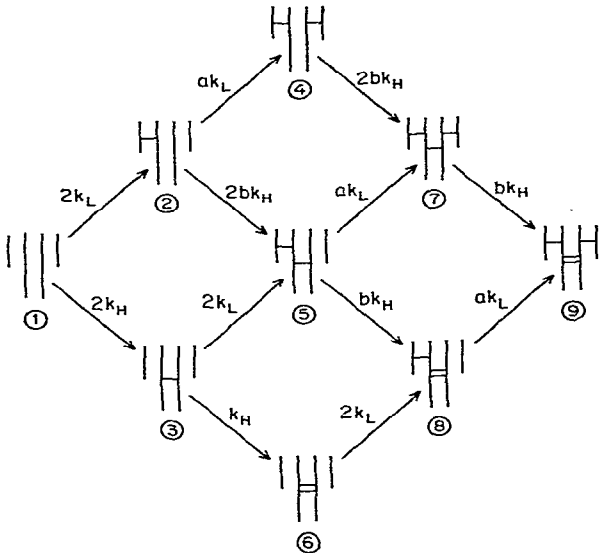

Fig. 3. Kinetic scheme for cooperative binding described by Model I: $k_{HH} = xk_{LH}$.

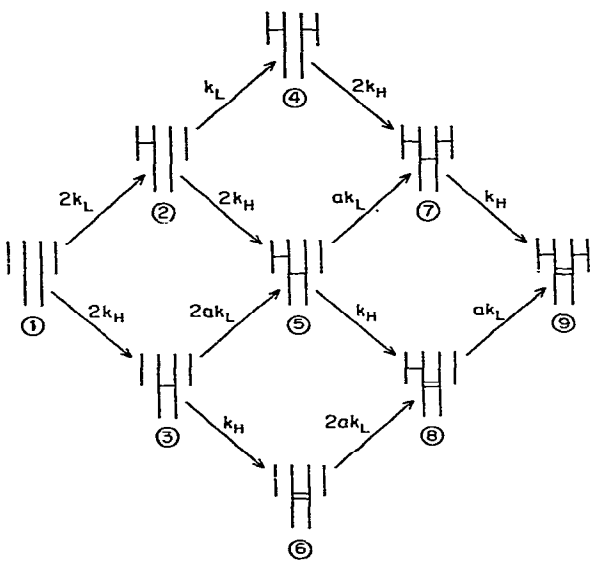

Fig. 4. Kinetic scheme for cooperative binding described by Model II: $k_{HH} = xk_{LH}$.

Model II is described by

$$k_{LH} = k_1 = k_3 ,$$
$$k_{HH} = k_2 = k_4 = k_6 = k_7 = k_8 = k_{11} = xk_1 ,$$
$$ak_{LH} = k_5 = k_9 = k_{10} = k_{12} = ak_1 . \quad (35)$$

The corresponding reaction scheme is shown in fig. 4. As can be seen in table 4, this model, with $x = 0.5$ and $a = 0.8$, agrees with experiment slightly better than the noncooperative model with $x = 0.5$. Fig. 2c shows the corresponding reaction profile. Since the improvement is so small, and a is so close to one, it appears premature to conclude that the experimental data indicate cooperativity. However, when more accurate and extensive information becomes available, the present formalism can be used to analyze the data.

5. Potential applications

Percy and coworkers [5–7] have performed a series of experimental studies of the covalent assembly of immunoglobulins which are similar to, albeit not identical to, the work of Beychok and coworkers. In addition, they analyzed these experiments within the framework of a model [4] which is different from that described in this paper. In this section we do not attempt to reanalyze their data. However, we wish to point out that our formalism appears to be an attractive alternative to theirs and that such a reanalysis would be of considerable interest.

Percy and coworkers present their experimental results as plots of fragment concentrations versus time. We can obtain corresponding plots using our formalism as follows. Our species concentrations, $c_l(t)$, are given as explicit functions of time involving the set rate constants $\{k_i\}$ (see Appendix). If we introduce a dimensionless time variable, say, $k_1 t$ then the species concentrations are functions only of this dimensionless time and the rate constant ratios k_i/k_1. To obtain the fragment concentrations from these species concentrations we cannot immediately use table 1 because Sears et al. [2,3] and Percy et al. [4–7] normalize their fragment concentrations differently. However, the fragment concentrations appropriate for comparison with the work of Percy et al. [4–7] can be obtained from table 1 by simply multiplying the entries for H_2, H_2L and H_2L_2 by 0.5.

For the purposes of illustration, in fig. 5 we present three plots which are directly comparable at the work of Percy and coworkers. These plots were obtained using noncooperative models with $x = 1$ (fig. 5a), $x = 0.5$ (fig. 5b) and $x = 0.4$ (fig. 5c). Figs. (5b) and (5c) were selected because they are strikingly similar to the theoretical plots shown in figs. 1 and 2 of ref. [4], respectively. This resemblance is remarkable in light of the very different physical conceptualizations on which the two sets of plots are based. In both cases, the agreement with experimental results is only semiquantitative. Although the plots are similar, the parameters giving rise to these plots are quite different; our $x = 0.5$ curve (fig. 5b) corresponds to their $x = 1$, and our $x = 0.4$ curve (fig. 5c) corresponds to their $x = 0.625$ (i.e. $p_{LH}/p_{HH} = 1.6$).

We believe that our work represents an attractive alternative to the model of Percy et al. [4] because our formulation directly parallels the way the experiments are actually performed. We use first-order rate equations to describe disulfide bond formation in the noncovalently assembled species in fig. 1. To obtain the concentration of a given fragment type, we first "break" the noncovalent interactions within each

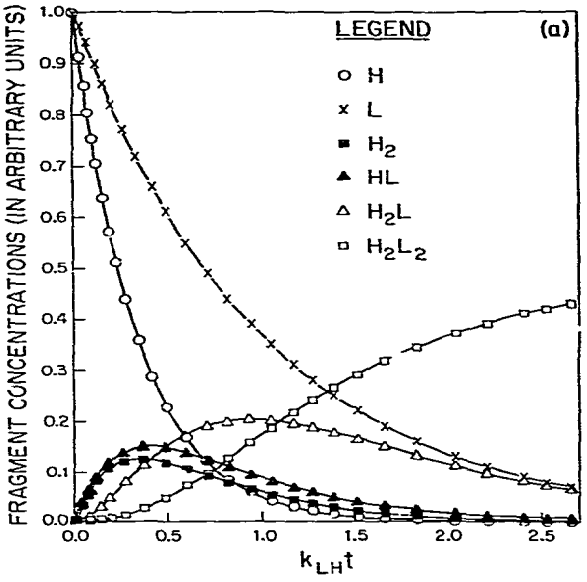

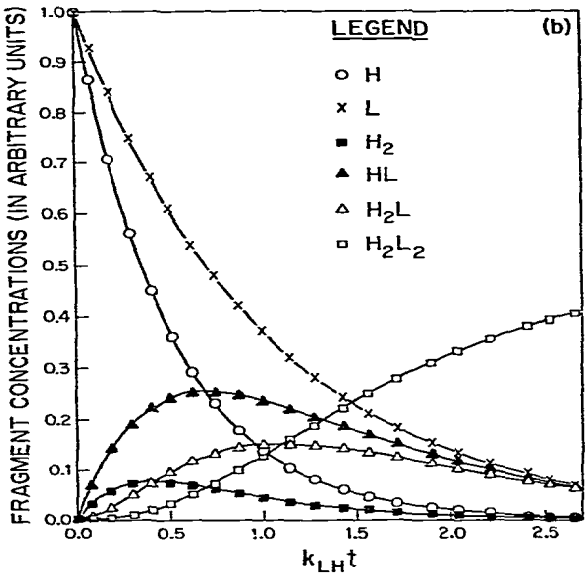

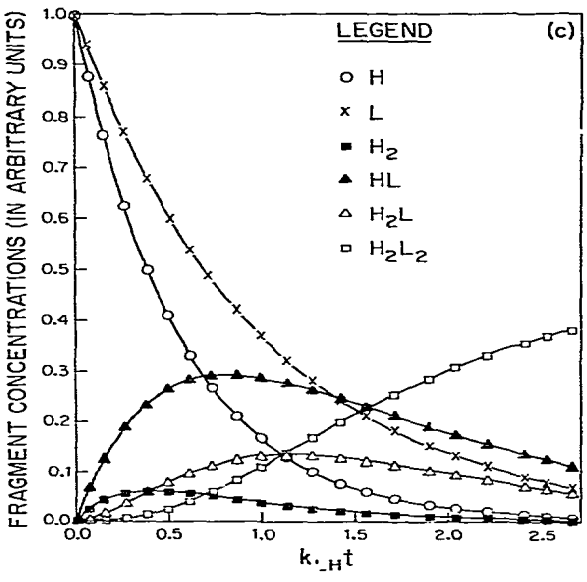

Fig. 5. Fragment concentrations versus $k_{LH}t$. a) All rate constants equal; b) Noncooperative, $x = 0.5$; c) Noncooperative, $x = 0.4$.

species and count the number of fragments produced of the type in question. By adding the contributions of all the species together, we obtain the total concentration of the fragment of interest. (See section 2.) In the model of Percy et al. [4] on the other hand, the fragment concentrations themselves obey second-order equations identical to those one would use to describe irreversible noncovalent assembly of immunoglobulins. In addition, our formalism yields analytic solutions for a general cooperative pathway while they have to

resort to a numerical solution even in the case of a noncooperative reaction scheme.

Since their model [4] can describe their experiments [5,6] only semiquantitatively, it would be of interest to reanalyze their data within the framework of our formalism to see if the agreement between theory and experiment could be improved. Of particular interest is whether such a reanalysis would yield a different physical picture of the pathway of of the covalent assembly in these systems.

Acknowledgements

We thank Professor Sherman Beychok for introducing ; to this problem. This work was supported by U.S. Public Health Service Grant HL-21483.

Appendix

Solutions to general equations

Note: $f(\nu) = e^{-\nu t}$, c_n is the concentration of species n in fig. 1.

$$c_1 = f(2k_1 + 2k_2), \qquad c_2 = c_2^0[f(k_3 + 2k_4) - f(2k_1 + 2k_2)], \qquad c_3 = c_3^0[f(2k_5 + k_6) - f(2k_1 + 2k_2)]$$

$$c_4 = \frac{-k_3 c_2^0}{2(k_7 - k_1 - k_2)} f(2k_1 + 2k_2) + \frac{k_3 c_2^0}{2k_7 - k_3 - 2k_4} f(k_3 + 2k_4) + c_4^0 f(2k_7),$$

$$c_5 = \frac{-4}{k_8 + k_9 - 2k_1 - 2k_2}\left(\frac{k_4 c_2^0}{2} + \frac{k_5 c_3^0}{2}\right) f(2k_1 + 2k_2)$$
$$+ \frac{2k_4 c_2^0}{k_8 + k_9 - k_3 - 2k_4} f(k_3 + 2k_4) + \frac{2k_5 c_3^0}{k_8 + k_9 - 2k_5 - k_6} f(2k_5 + k_6) + c_5^0 f(k_8 + k_9),$$

$$c_6 = \frac{-k_6 c_2^0}{2(k_{10} - k_1 - k_2)} f(2k_1 + 2k_2) + \frac{k_6 c_3^0}{2k_{10} - 2k_5 - k_6} f(2k_5 + k_6) + c_6^0 f(2k_{10}),$$

$$c_7 = \frac{-1}{k_{11} - 2k_1 - 2k_2}\left[\frac{k_7 c_2^0}{k_7 - k_1 - k_2} + \frac{4k_8}{k_8 + k_9 - 2k_1 - 2k_2}\left(\frac{k_4 c_2^0}{2} + \frac{k_5 c_3^0}{2}\right)\right] f(2k_1 + 2k_2)$$
$$+ \frac{2c_2^0}{k_{11} - k_3 - 2k_4}\left(\frac{k_3 k_7}{2k_7 - k_3 - 2k_4} + \frac{k_4 k_8}{k_8 + k_9 - k_3 - 2k_4}\right) f(k_3 + 2k_4)$$
$$+ \frac{2c_3^0}{k_{12} - 2k_5 - k_6}\left(\frac{k_9 k_5}{k_8 + k_9 - 2k_5 - k_6} + \frac{k_{10} k_6}{2k_{10} - 2k_5 - k_6}\right) f(2k_5 + k_6)$$
$$+ \frac{2k_7 c_4^0}{k_{11} - 2k_7} f(2k_7) + \frac{k_8 c_5^0}{k_{11} - k_8 - k_9} f(k_8 + k_9) + c_7^0 f(k_{11}),$$

$$c_8 = \frac{-2}{k_{12}-2k_1-2k_2}\left[\frac{2k_9}{k_8+k_9-2k_1-2k_2}\left(\frac{k_4c_2^0}{2}+\frac{k_5c_3^0}{2}\right)+\frac{k_{10}k_6c_3^0}{2(k_{10}-k_1-k_2)}\right]f(2k_1+2k_2)$$
$$+\frac{2k_9k_4c_2^0}{(k_{12}-k_3-2k_4)(k_8+k_9-k_3-2k_4)}f(k_3+2k_4)$$
$$+\frac{2c_3^0}{k_{12}-2k_5-k_6}\left[\frac{k_9k_5}{k_8+k_9-2k_5-k_6}+\frac{k_{10}k_6}{2k_{10}-2k_5-k_6}\right]f(2k_5+k_6)$$
$$+\frac{k_9c_5^0}{k_{12}-k_8-k_9}f(k_8+k_9)+\frac{2k_{10}c_6^0}{k_{12}-2k_{10}}f(2k_{10})+c_8^0f(k_{12}),$$

$$c_9 = 1-(c_1+c_2+c_3+c_4+c_5+c_6+c_7+c_8),$$

$$c_2^0 = \frac{-2k_1}{k_3+2k_4-2k_1-2k_2}, \qquad c_3^0 = \frac{-2k_2}{2k_5+k_6-2k_1-2k_2}, \qquad c_4^0 = \frac{k_1k_3}{(2k_7-k_3-2k_4)(k_7-k_1-k_2)},$$

$$c_5^0 = \frac{4}{k_8+k_9-2k_1-2k_2}\left(\frac{k_1k_4}{k_8+k_9-k_3-2k_4}+\frac{k_2k_5}{k_8+k_9-2k_5-k_6)}\right)$$

$$c_6^0 = \frac{k_2k_6}{(2k_{10}-2k_5-k_6)(k_{10}-k_1-k_2)},$$

$$c_7^0 = \frac{1}{k_{11}-2k_1-2k_2}\left[\frac{k_7c_2^0}{k_7-k_1-k_2}+\frac{4k_8}{k_8+k_9-2k_1-2k_2}\left(\frac{k_4c_2^0}{2}+\frac{k_5c_3^0}{2}\right)\right]$$
$$-\frac{2c_2^0}{k_{11}-k_3-2k_4}\left(\frac{k_3k_7}{2k_7-k_3-2k_4}+\frac{k_4k_8}{k_8+k_9-k_3-2k_4}\right)$$
$$-\frac{2k_5k_8c_3^0}{(k_{11}-2k_5-k_6)(k_8+k_9-2k_5-k_6)}-\frac{2k_7c_4^0}{k_{11}-2k_7}-\frac{k_8c_5^0}{k_{11}-k_8-k_9},$$

$$c_8^0 = \frac{2}{k_{12}-2k_1-2k_2}\left[\frac{2k_9}{k_8+k_9-2k_1-2k_2}\left(\frac{k_4c_2^0}{2}+\frac{k_5c_3^0}{2}\right)+\frac{k_6k_{10}c_3^0}{2(k_{10}-k_1-k_2)}\right]$$
$$-\frac{2c_2^0k_4k_9}{(k_{12}-k_3-2k_4)(k_8+k_9-k_3-2k_4)}-\frac{2c_3^0}{k_{12}-2k_5-k_6}\left(\frac{k_5k_9}{k_8+k_9-2k_5-k_6}+\frac{k_6k_{10}}{2k_{10}-2k_5-k_6}\right)$$
$$-\frac{k_9c_5^0}{k_{12}-k_8-k_9}-\frac{2k_{10}c_6^0}{k_{12}-2k_{10}}.$$

References

[1] D.W. Sears, J. Mohrer and S. Beychok, Proc. Natl. Acad. Sci. U.S.A. 72 (1975) 353.
[2] D.W. Sears, A.R. Kazin, J. Mohrer, F. Friedman and S. Beychok, Biochemistry 16 (1977) 2016.
[3] D.W. Sears and S. Beychok, Biochemistry 16 (1977) 2026.
[4] J.R. Percy, M.E. Percy and K.J. Dorrington, J. Biol. Chem. 250 (1975) 2398.
[5] M.E. Percy, R. Baumal, K.J. Dorrington and J.R. Percy, Can. J. Biochem. 54 (1976) 675.
[6] J.R. Percy, M.E. Percy and R. Baumal, Can. J. Biochem. 54 (1976) 688.
[7] M.E. Percy, L. Chang, C. Demoliou and R. Baumal, Can. J. Biochem. 57 (1978) 279.